



## Short communication

## Effects of impurities on the degradation and long-term stability for solid oxide fuel cells

Teruhisa Horita<sup>a,\*</sup>, Haruo Kishimoto<sup>a</sup>, Katsuhiko Yamaji<sup>a</sup>, Manuel E. Brito<sup>a</sup>, Yueping Xiong<sup>a</sup>, Harumi Yokokawa<sup>a</sup>, Yuichi Hori<sup>b</sup>, Itaru Miyachi<sup>b</sup><sup>a</sup> National Institute of Advanced Industrial Science and Technology (AIST), Japan<sup>b</sup> Kyocera Corporation, R&D Center, Japan

## ARTICLE INFO

## Article history:

Received 19 September 2008

Received in revised form 28 October 2008

Accepted 29 October 2008

Available online 13 November 2008

## Keywords:

SOFC

Degradation

Durability

Stack

Impurity

SIMS

## ABSTRACT

The effect of impurities on the degradation of performances was investigated for the flatten tube type SOFC stack. The durability tests of 20-cells stack were conducted at 750 °C (1023 K) with dry H<sub>2</sub> for more than 5000 h under a constant current density of 0.3 A cm<sup>-2</sup>. The voltage loss showed a linear relationship between voltage loss and operation time (about 1.5%/1000 h). The ohmic resistance increased with operation time while the polarization resistance showed constant values. After the long-term operation test, the concentration levels of impurities were measured at cathode and interlayer by secondary ion mass spectrometry (SIMS). The concentrations of several elements were successfully determined in ppm levels. The concentrations of several elements increased with operation time (Na, Al, Si, and Cr), which suggested the transports and depositions on the cell component surface. The increase of resistance and impurity concentration at the interlayer were estimated from the literature data and SIMS impurity analysis.

© 2008 Elsevier B.V. All rights reserved.

## 1. Introduction

In order to operate solid oxide fuel cells (SOFCs) for long-term with stable performance, the degradation factors must be clarified at component materials and interfaces. Among many degradation factors, several authors pointed out that impurities in the components (raw materials) can affect the degradation of performance and long-term stability: impurities could condense at anode/electrolyte interface during operation (such as Si and alkaline), and they increased the polarization resistance [1–4]. In other cases, some authors reported the degradation by impurity gases, which could deposit and react with the cell components: Cr poisoning is a typical phenomenon by the supply of impurity gases [5,6]. Several poisoning elements (H<sub>2</sub>S, CH<sub>3</sub>SH, COS, Cl<sub>2</sub>, and siloxane) have examined at anode [7]. Degradations of single cells by the impurities were well determined with sensitive analysis of electrochemical measurements. However, only a few data are available on the concentration levels of impurities in real stacks, and effects of those impurities on the degradation have not been clarified yet. The present study aims to clarify the effects of impurities

of gases (air and fuels) on the degradation of performances for real stacks. Because the stacks are composed of several kinds of outer components, the degradation should also be considered for the impurities from them (outer components: gas manifold, thermal insulating materials, metallic gas supply pipes, etc.). To clarify the effect of impurities on the degradation in real SOFC stacks, the SOFC reliability project has been initiated under the SOFC system development project by the New Energy Development Organization (NEDO), Japan in 2005–2008. The durability of four different types of stacks/modules (100 W–1 kW) was examined under constant current density with an operation time of 5000–10,000 h [8–10]. After the long-term durability tests, the chemical reaction was especially investigated at the cell components and interfaces of different materials.

To detect the concentration levels of impurities (less than 1000 ppm) and reaction products in the cell components after long-term operation, secondary ion mass spectrometry (SIMS) technique has been applied to the samples of real stacks. We succeed in determining the concentration levels of several impurity elements at each cell component for four types of stacks/modules. Some key phenomena associated with cell degradation were extracted from the impurity level analysis [9,10].

In this report, effects of concentration levels of impurities on the degradation of performance were examined at the flatten tube type stack (some 100 W stack). The concentration levels of impurity

\* Corresponding author at: AIST Central 5, Higashi 1-1-1, Tsukuba, Ibaraki 305-8565, Japan. Tel.: +81 29 861 9362; fax: +81 29 861 4540.

E-mail address: [t.horita@aist.go.jp](mailto:t.horita@aist.go.jp) (T. Horita).

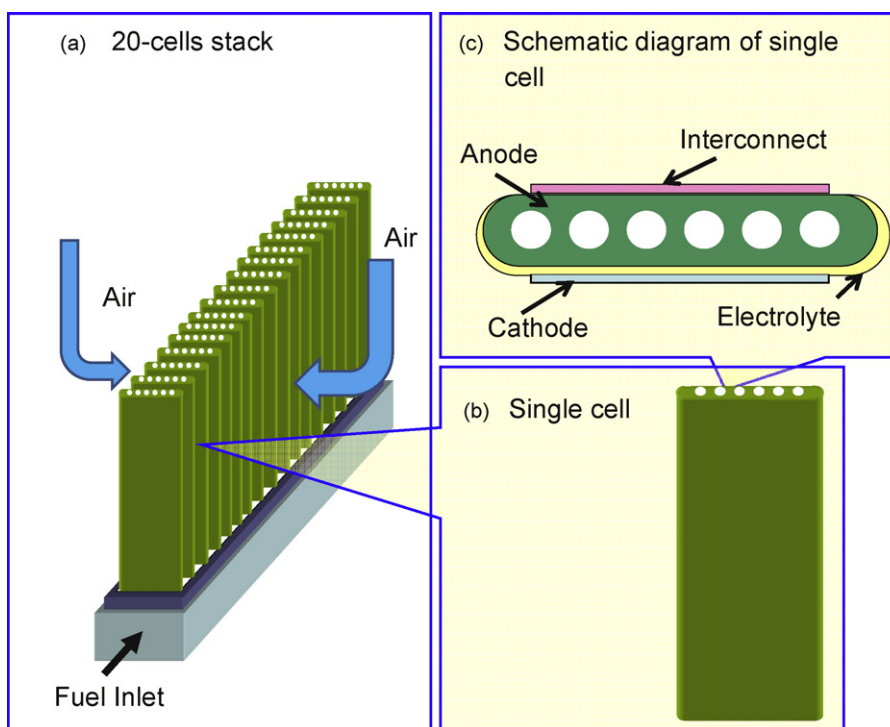


Fig. 1. Schematic diagram of flatten tube-type SOFCs. (a) Schematic diagram of 20 cells stack, (b) single cell, (c) schematic drawing of single cell.

were compared with different operation times (for 24–8000 h) at cathode and interlayer. Some key impurity elements and related degradation factors were considered by assuming a model between impurities and resistance.

## 2. Experimental

### 2.1. Sample

The flatten tube-type stack was made by Kyocera Corporation Ltd., Kagoshima, Japan. Fig. 1 shows a schematic diagram of flatten tube stack (a), single cell (b), and schematic drawing of cross-section of single cell (c). The stack is composed of 20 single cells with electrically in-series connection. In the single cell, porous Ni-oxide mixture (cermet) is the supported tube with fuel flow holes. On the supported tube, a thin porous Ni-ZrO<sub>2</sub> anode was coated on the surface. Over the anode layer, a thin Y<sub>2</sub>O<sub>3</sub>-stabilized ZrO<sub>2</sub> (YSZ) electrolyte and LaCrO<sub>3</sub> interconnect were coated with dense structures. On the dense YSZ electrolyte, CeO<sub>2</sub>-based interlayer was coated to avoid chemical reaction between YSZ and cathode materials. Over the interlayer, porous LaFeO<sub>3</sub>-based cathode was fabricated.

### 2.2. Long-term durability test

The durability test was conducted under a constant current density (0.3 A cm<sup>-2</sup>) at 750 °C (1023 K) for more than 5000 h. The fuel was dry H<sub>2</sub> with a fuel utilization of 75%, while air was supplied as an oxidant. The voltage value was measured as a function of operation time, and the decrease rate of voltage was calculated from the initial value of voltage (decrease rate %:  $(E^0 - E)/E^0 \times 100$ ,  $E$  is the measured voltage,  $E^0$  is the initial voltage). To determine the ohmic resistance and polarization, AC impedance analyses were performed for single cell.

### 2.3. Impurity analysis

After the long-term operation test under constant current density, the concentration levels of impurities were measured by SIMS. We selected Cs<sup>+</sup> or O<sub>2</sub><sup>+</sup> as a primary beam and the secondary negative or positive ions were measured as a function of sputtering time. The acceleration voltages of primary ions were set as 10–12.5 kV with primary beam current of 10–50 nA. To determine the concentration of impurities, calibration curves of concentration were made between the secondary ion signal intensity and corresponding concentration of each element. The exact concentration levels were determined from the relative sensitive factors of each element by using standard materials.

## 3. Results

### 3.1. Long-term durability test of flatten tube stack

Fig. 2 shows voltage change of flatten tube stack under constant current density (0.3 A cm<sup>-2</sup>) at fuel utilization of 75% (dry H<sub>2</sub> flow).

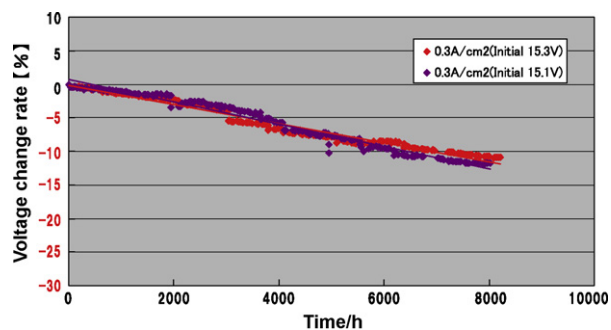


Fig. 2. Voltage change of 20-cells stack under constant current flow (negative values are voltage loss from the initial value).

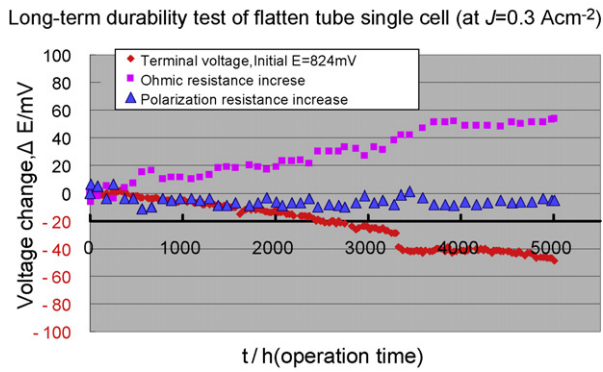


Fig. 3. Voltage change of single cell under constant current flow (negative values are voltage loss from the initial value).

The Y-axis indicates the voltage change rates from the initial values ( $-(E^0 - E)/E^0 \times 100$ ,  $E$  is the measured voltage,  $E^0$  is the initial voltage). The negative value indicates the decrease of voltages from the initial values (that is, the degradation of stack voltage from the initial value). The voltage loss shows linear decrease trends with time for both two stacks, which suggests the continuous increase of resistance during operation. The average voltage degradation rate was calculated to be 1.5–1.6%/1000 h in these stacks.

To clarify the degradation of stack performance, the impedance analyses were examined for single cells under constant current density. Fig. 3 shows the change of the terminal voltage for single cell (diamond symbol), the ohmic resistance (square symbol), and the polarization resistance (triangle symbol) under constant current density. The ohmic resistance and polarization resistance was converted to the voltage under constant current density ( $J=0.3 \text{ A cm}^{-2}$ ). Thus, an increase of voltage indicates the increase of resistance at each component under a constant current density. The ohmic resistance increases with time while the polarization resistance shows constant values. It is suggested that the terminal voltage loss was mainly ascribed to the ohmic resistance increase. This ohmic resistance increase can be due to the formation of high resistance materials in the components and at the interfaces. The increase of ohmic resistance is about 50 mV at 5000 h. This corresponds to the voltage loss of 50 mV from the initial value (824 mV). The degradation rate is calculated to be about 6%/5000 h (1.2%/1000 h).

### 3.2. Impurity analysis of flatten tube cell

To clarify the effects of impurities on the stack performances, the concentration levels of several elements were measured for samples of different operation times by using SIMS. Fig. 4 shows example of SIMS depth profiles of positive ions around interlayer/electrolyte interface after 5000 h operation (primary ion:  $\text{O}_2^+$ ). The  $\text{CeO}_2$ -based interlayer is identified as the higher signal counts of  $\text{Ce}^+$  and some other elements. In the YSZ electrolyte part, the higher signal counts of  $\text{Zr}^+$  is identified. From the SIMS signal counts at the interlayer, several kinds of minor elements are identified, such as Si, Sr, Cr, and Al. These elements are thought to be impurities, and they come from the thermal insulating materials, gas supply tubes, and other components.

The SIMS signals for several impurity elements were converted to the concentration by using the relative sensitive factors (the relationship between SIMS secondary ion intensity and the concentration). Fig. 5 shows the concentration levels of several kinds of impurities observed at cathode surface. The bars in the figure indicate the concentration of several kinds of impurities at differ-

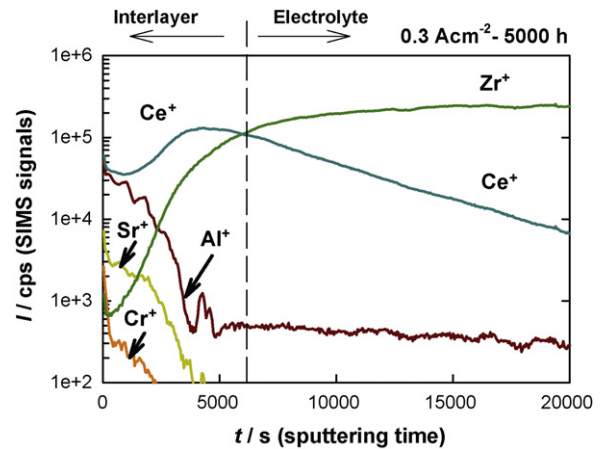


Fig. 4. SIMS depth profiles of some elements at interlayer/electrolyte interface (sample: interlayer/electrolyte, operation at  $0.3 \text{ A cm}^{-2}$  for 5000 h).

ent operation times. From left to right hand side, the bar indicates the concentration of each element operation time at 24 h, 3000 h, 5000 h, and 8000 h. Thus, we can identify the concentration change trends by comparing the heights of these bars. Several elements show the increase of concentrations with operation time, such as Na, Al, Si, and Cr. These elements can be supplied from air, and condensed on the cathode surface during the long-term operation. The source of these elements has not been clarified yet. However, one of the sources of Na, Al, and Si can be thermal insulating materials, which covered the whole stack in the furnace. The impurity of Cr can be supplied from the stainless steel pipe or pre-heater. Among impurity elements, a relatively high concentration of Si was observed at cathode; from about 100 ppm at 24 h to 400 ppm after 8000 h.

Fig. 6 shows the concentration levels of several kinds of impurities observed at the interlayer surface (the analyzed surface was without cathode materials where the interlayer was exposed to the air). The bars are the same configurations in Fig. 5. Among several kinds of impurities, the concentration of Si increased with time, which suggests the condensation of Si or reaction products formation during the long-term operation. The concentration levels of Si change from 165 ppm (24 h) to about 910 ppm (8000 h). This increase of Si concentration seems to be relatively large compared

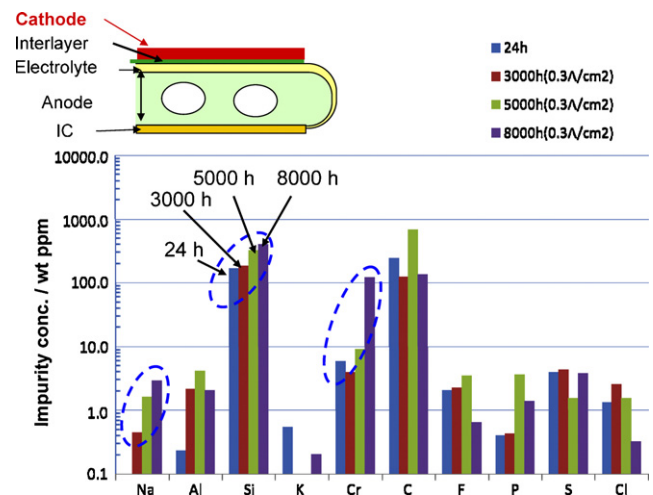


Fig. 5. Concentration of several kinds of impurity elements at cathode for operation time of 24 h, 3000 h, 5000 h, and 8000 h (operation under constant current of  $0.3 \text{ A cm}^{-2}$  at  $750^\circ \text{C}$ ).

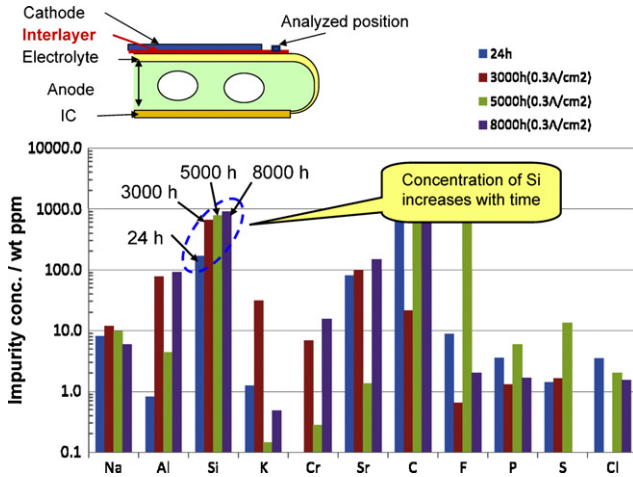


Fig. 6. Concentration of several kinds of impurity elements at interlayer for operation time of 24 h, 3000 h, 5000 h, and 8000 h (operation under constant current of  $0.3 \text{ A cm}^{-2}$  at  $750^\circ\text{C}$ ).

with the other elements. Thus, the concentration of Si can affect the increase of resistance at the interlayer.

#### 4. Discussion

##### 4.1. Impurity concentration (Si) and increase of resistance at the interlayer

The increase of Si concentration in the interlayer and related increase of resistance was considered. Since the interlayer was composed of  $\text{CeO}_2$ -based oxide, the effects of Si on the conductivity of  $\text{CeO}_2$  can be estimated from the literature data. Fig. 7 shows summary of reported data of  $\text{SiO}_2$  concentration and resistance of Gd-doped  $\text{CeO}_2$  (GDC) up to 1500 ppm [11,12]. We can assume that the parabolic increase of resistance as a function of  $\text{SiO}_2$  concentration:  $R^2$  is proportional to the  $\text{SiO}_2$  concentration. This phenomenon is empirical result. One possible reason for the parabolic relationship is the growth of insulating  $\text{SiO}_2$ -based layer growth. If the thickness of insulating layer is proportional to the concentration of  $\text{SiO}_2$ , a parabolic relationship can be valid between  $\text{SiO}_2$  concentration and resistance at the interlayer. In the future, we will report exact analysis of Si impurity effects. The  $\text{SiO}_2$  concentrations of the  $\text{CeO}_2$ -based interlayer at certain operation times are measured by SIMS impurity analyses (Fig. 6). From the SIMS impurity analysis, we

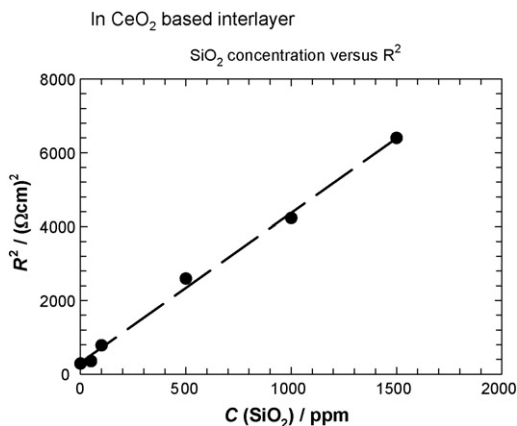


Fig. 7. Relationship between  $\text{SiO}_2$  concentration and resistance of doped  $\text{CeO}_2$  (data comes from Refs. [11,12]).

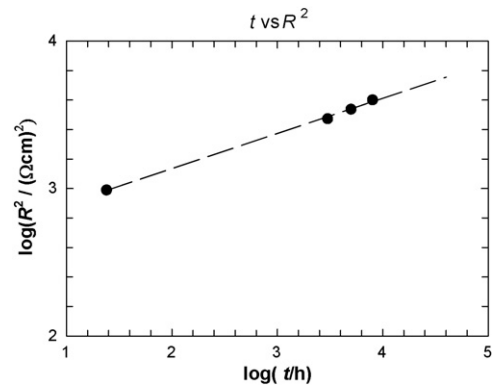


Fig. 8. Relationship between operation time and resistance of  $\text{CeO}_2$  interlayer.

can estimate the relationship between resistance of GDC interlayer and operation time. In order to evaluate the resistance for long-term operation (for more than 10,000 h operation), the logarithm of resistance ( $R^2$ : this is proportional to the Si concentration) is plotted as a function of the logarithm of operation time, as follows:

$$\log(R^2) = A \times \log t + B \tag{1}$$

where  $A$  and  $B$  are the constants,  $t$  is the operation time of the stack. In Fig. 8, the estimated resistance was plotted as a function of operation time. The circle symbol indicates the estimated resistance based on the observed Si concentration and operation time, and broken line indicates the fitting of the measured data. From the fitting line of this graph, the estimated resistance of GDC layer after 40,000 h operation is calculated to be  $75 \text{ } \Omega\text{cm}$  ( $31 \text{ } \Omega\text{cm}$  at 24 h). Thus, the ohmic resistance increases about 2.5 times larger than the initial values. From the fitting line of  $R^2$  versus operation time (Fig. 8), the following equation can be obtained:  $R^2 = A \times t^{0.32} + B$  ( $A$  and  $B$  are the constants). This indicates the lower operation time dependence of the resistance. So far, there is no theoretical explanation on the relationship between  $R^2$  and operation time. We are now examining the physical meaning of this dependence. Since the thickness of interlayer is very thin (less than  $5 \text{ } \mu\text{m}$ ), the contribution to the increase of single cell resistance is not so significant. This assumption is roughly consistent with the increase of ohmic resistance of the single cell measured in Fig. 3, although the increase rate by Si impurity is not clear. This is one example of the increase in the resistance by the impurity of Si at the interlayer. To understand the effects of impurities on the degradation in stack, we have to expand this method to the other kinds of impurity elements and other component parts. In the near future, we will examine the effects of impurity concentrations on the polarization resistances at the cathode/electrolyte interfaces.

##### 4.2. Durability and reliability of flatten tube stacks

In the first durability test of flatten tube stacks, the average degradation rates of stack voltage were 1.5–1.6%/1000 h at  $0.3 \text{ A cm}^{-2}$  for two stacks. A linear decrease of voltage was observed for both stacks. Thus, the degradation mechanisms are similar between these two stacks. When estimating the voltage loss of stack, the increase of resistance occurred at the single cell component interfaces as well as the connection metal/single cell interfaces. Some modifications were made at the interlayer of single cells and cell connection at metal/single cell interfaces. The stack degradation was reduced to be 0.9%/1000 h at  $0.3 \text{ A cm}^{-2}$  for the second durability test (in the modified stack). This was mainly due to a good electrical connection at the cathode/interlayer/electrolyte interfaces and the metal/single cell

interfaces. For the impurity analysis of the modified cells, we observed somewhat decrease of the Si concentration at the inter-layer: 660 ppm at 3000 h for 1st stack and 560 ppm at 4000 h for the modified stack. This indicates that the decrease of Si concentration can partly improve the stack performance. However, it has not been clarified the exact relationship between the impurity concentrations and the increase of resistance in single cells and stacks. To fabricate more reliable stack for the long-term operation, we are planning to improve the evaluation method for the life time of stack. Accelerating testing for evaluating the life time of stack will be presented to evaluate the durability of the stacks.

## 5. Conclusion

The effect of impurities on the degradation was investigated for the flatten tube-type SOFC stack. The durability test of 20-cells stack was conducted at 750 °C with dry H<sub>2</sub> under a constant current density of 0.3 A cm<sup>-2</sup> more than 5000 h. The voltage loss showed the linear relationship between voltage loss rate and operation time (about 1.5%/1000 h). The ohmic resistance increased with operation while the polarization resistance showed constant values. After the long-term operation test, the concentration levels of impurities were measured by SIMS. The concentrations of several elements were successfully determined in ppm levels at cathode and inter-layer surfaces. The concentrations of several elements increased with operation time (Na, Al, Si, and Cr), which suggested the trans-

ports and depositions of impurities on the cell components. The increase of resistance and impurity concentration were evaluated for some specific elements in the flatten tube-type SOFC stack.

## Acknowledgements

Part of this work was supported by the New Energy Development Organization (NEDO) under the SOFC system development project. The authors are very grateful to the organization.

## References

- [1] Y.L. Liu, C. Jiao, *Solid State Ionics* 176 (2005) 435–442.
- [2] Y.L. Liu, S. Primdahl, M. Mogensen, *Solid State Ionics* 161 (2003) 1–10.
- [3] M.S. Schmidt, K. Vels Hansen, K. Norrman, M. Mogensen, *Solid State Ionics* 179 (2008) 1436–1441.
- [4] A. Hagen, Y.L. Liu, R. Barfod, P.V. Hendriksen, *J. Electrochem. Soc.* 155 (10) (2008) B1047–B1052.
- [5] Y. Matsuzaki, I. Yasuda, *Solid State Ionics* 132 (2000) 271–278.
- [6] S.P. Jiang, S. Zhang, Y.D. Zhen, *J. Electrochem. Soc.* 153 (1) (2006) A127–A134.
- [7] K. Haga, S. Adachi, Y. Shiratori, K. Itoh, K. Sasaki, *Solid State Ionics* 179 (2008) 1427–1431.
- [8] H. Yokokawa, T. Horita, N. Sakai, K. Yamaji, M.E. Brito, Y.-P. Xiong, H. Kishimoto, *Solid State Ionics* 177 (2006) 3193–3198.
- [9] H. Yokokawa, T. Watanabe, A. Ueno, K. Hoshino, *ECS Trans.* 7 (1) (2007) 133–140.
- [10] H. Yokokawa, T. Horita, K. Yamaji, H. Kishimoto, Y.P. Xiong, M.E. Brito, *Proceedings of 8th European SOFC Forum, CD-ROM version, 2008, B1004.*
- [11] T.S. Zhang, J. Ma, Y.Z. Chen, L.H. Luo, L.B. Kong, S.H. Chan, *Solid State Ionics* 177 (2006) 1227–1235.
- [12] J.A. Lane, J.L. Neff, G.M. Christie, *Solid State Ionics* 177 (2006) 1911–1915.